Staff Papers

STABILITY OF PIPELINES IN TRENCHES

R.H. Wilkinson (Hydraulics Research)
A.C. Palmer (Andrew Palmer and Associates)
J.W. Ells (British Petroleum)
E. Seymour (Woodside Petroleum)
N. Sanderson (Kvaerner Engineering)

Offshore Oil and Gas Pipeline Technology Seminar
Stavanger 1988

Introduction

The need for the study reported in this paper was originally identified during the engineering of the 24-inch West Sole gas pipeline in 1980. The West Sole field is characterised by high currents that generally flow across the pipeline route. It had been found that it was not practicable to apply adequate concrete coating to stabilise the 24-inch pipeline on the seabed without incurring installation and manufacturing difficulties. It was therefore decided to achieve stability by trenching the pipeline. Previous experience of pipeline burial in the West Sole field by the then commonly used jetting technique had been found to be generally unsatisfactory in the very stiff boulder clays that predominated. BP subsequently trenched the 24-inch pipeline in a 1 m deep trench, using the post-ploughing technique and following a full-scale offshore trial in seabed materials representative of the proposed pipeline route. This was the first application of post-ploughing in the North Sea.

The plough leaves the pipe in an open V-shaped trench with sides at 30° to the horizontal. The pipe is initially exposed, although sediment transport tends to backfill the trench. The lack of adequate data on the hydrodynamic loading on a pipeline in a trench resulted in a number of conservative assumptions being made in the stability assessment of the 24-inch pipeline.

During the subsequent design work for the North Sea Gas Gathering Pipeline (NSGGP), performed by BP on behalf of its partners Mobil and British Gas in 1981, the designer was faced by the same problem. The requirement was to stabilise large-diameter pipelines, without using excessively thick concrete coating and incurring the associated installation difficulties and costs.

The capability of the trenching technique had been demonstrated in the West Sole field. It followed that it had to be considered a viable option for the NSGGP, but that the stability assessment ought to allow for the effect of the trench on the hydrodynamic force experienced by the pipe. Hydraulics Research was commissioned to carry out model tests to obtain the data. The work had to be carried out rapidly, to allow the NSGGP project schedule to be kept, and the test results were applied as soon as they became available.

The intention of the stability research was to optimise the concrete coating requirements, and to meet the following objectives:

1 to minimise the concrete coating thickness required to achieve stability in an open trench during the design lifetime;

2 to ensure stability on the seabed during the installation season; and

3 to allow installation by conventional lay methods.

During the course of the programme, Woodside Petroleum identified the same need for data on hydrodynamic forces on a pipeline in a ploughed trench, for the stability design of the 40-inch North Rankin pipeline. It was agreed that Woodside would join the programme, and that there should be additional tests, on the effects of spoil on the trench sides, of partial burial, and of spanning within a trench.

A trench has a two-fold stabilising effect. It shelters the pipe, and much reduces hydrodynamic forces. A second effect is equally important. A pipeline in a trench has a greatly enhanced lateral resistance, because it can only move by sliding up the side of the trench (or deforming the trench side). This factor is examined at the end of the paper.

Experimental procedure

The tests were carried out in the Hydraulic Research pulsating water tunnel, which can produce rectilinear oscillatory flow of variable period and orbit length in a rectangular test section 2.3 m high, 0.5 m wide and 9.1 m long. A maximum oscillatory velocity of 1.8 m/s can be produced, and a unidirectional current of 0.6 m/s can be superimposed on the oscillatory flow. The flow path in the tunnel is a closed horizontal loop. The oscillatory flow is forced by the motion of a piston, which can be programmed to be regular or random with a selected frequency content in the period range 3 to 15 seconds. The total flow velocity in the working section was measured by a 10 cm discus head electromagnetic flow meter.

Each trench section was obtained by constructing a false floor in the tunnel. The plywood floor extended over the full length of the tunnel working section, and a gradual transition to the original bed level was made at each bend.

The model pipeline was a piece of 273 mm diameter smooth PVC pipe, mounted horizontally across the tunnel at floor level at the midpoint of the working section. In order to avoid distortion of the force measurements by the boundary layers on the tunnel walls, the test pipe had three sections, a centre section 148 mm long flanked by two side sections 176 mm long. The dummy side sections were fasted to the tunnel walls. The centre section was coaxially mounted on a steel tube, which passed through a soft watertight gland in the tunnel wall: the tube formed the suspension for force measurement. The gaps between the centre and side sections were 0.75 to 1 mm wide: previous work had shown the effect of gaps of this order to be negligible. The small gap between the bed and the test pipe was sealed by foam rubber to prevent leakage.

An inductive transducer measured the vertical and horizontal deflections of the end of the tube on which the measurement section of the pipe was mounted. The deflections were linearly proportional to the corresponding forces. The natural frequency of the system was approximately 50 Hz, well above the flow oscillation frequency, but as an extra precaution the free end of the cantilever was damped in oil and the output was electronically filtered at 25 Hz. The entire force measurement system was mounted on a concrete plinth completely isolated from the tunnel structure, to ensure that the vibrations from the flow generation did not contaminate the force signals. The system was statically calibrated before each test, and the calibration was found to be consistent and repeatable. Reference 1 gives further details of the experimental scheme.

The force and velocity signals were digitised at between 12 and 24 Hz, the rate being adjusted and synchronised to give 2^n samples for each flow cycle, to optimise the Fast Fourier Transform (FFT) harmonic analysis of the data.

The blockage ratio was about 0.12. Previous work in the tunnel indication that the corresponding force correction factor is 1.01.

Data analysis

It was decided to base the data analysis on the Morison equation for forces on slender bodies in unsteady flow. The Morison equation is known not to be a good representation of the forces in unsteady flow, but is widely used in offshore pipeline engineering because it is the only reasonably straightforward theoretical model available, though Grace[2] has convincingly argued that a force-coefficient approach is simpler and at least as accurate. A decision to express the results in terms of Morison coefficients has the advantage that it allows straightforward comparison with measured coefficients for untrenched pipelines.

The Morison equation is:

$$F_x = \tfrac{1}{2}\rho C_D D u|u| + (\pi/4)\rho D^2 C_M \, du/dt \qquad (1)$$

$$F_y = \tfrac{1}{2}\rho C_L D u^2 \qquad (2)$$

where

- F_x is the horizontal force per unit length of pipeline,
- ρ is the density of the water,
- C_D is a drag coefficient,
- C_L is a lift coefficient,
- C_M is an inertia coefficient,
- D is the outside diameter of the pipeline,
- u is the instantaneous velocity of the water,
- du/dt is the instantaneous horizontal acceleration of the water,
- $|u|$ is the absolute value of u.

The horizontal acceleration du/dt in a plane flow is strictly given by

$$\frac{du}{dt} = \frac{\partial u}{\partial t} + u\frac{\partial u}{\partial x} + v\frac{\partial u}{\partial y} \qquad (3)$$

where x and y are horizontal and vertical coordinates, and v is the vertical velocity. In applications, it is usual to ignore the convective terms $u\,\partial u/\partial x$ and $v\,\partial u/\partial y$: Sarpkaya and Isaacson[3] examine the question in detail, and argue that there is some justification for neglecting the convective terms. In the pulsating water tunnel, the convective acceleration is in any case zero.

The values of C_D and C_M were determined by comparing the coefficients of the first harmonic of a Fourier series decomposition of the Morison's equation with those of the data. In a pure oscillatory flow

$$u(t) = U \cos \omega t \tag{4}$$

and the Fourier series decomposition of (1) is

$$F_x(t)/\tfrac{1}{2}\rho DU^2 = C_D(8/3\pi)[\cos\omega t - (1/5)\cos 3\omega t + ..] - C_M(\pi D\omega/2U)\sin\omega t \tag{5}$$

The data were nondimensionalised and passed through an FFT, so that

$$F_x(t)/\tfrac{1}{2}\rho DU^2 = a_o + \sum_n (a_n\cos n\omega t + b_n\sin n\omega t) \tag{6}$$

and values for C_D and C_M were obtained by comparing the sin t and cos t coefficients of the data (6) and the Morison equation (5), so that

$$C_D = (3\pi/8)a_1 \tag{7}$$

and

$$C_M = -(2U/\pi D\omega)b_1 \tag{8}$$

When a steady current component V is superimposed on the oscillatory current

$$u(t) = V + U \cos\omega t \tag{9}$$

the equations are modified. When V>U, so that the flow never reverses, the Fourier decomposition of the Morison equation becomes

$$F_x(t)/\tfrac{1}{2}\rho DU^2 = C_D[(\alpha^2+\tfrac{1}{2}) + 2\alpha\cos\omega t + \tfrac{1}{2}\cos 2\omega t]$$

$$- C_M(\ D\ /2U)\sin\ t \qquad (10)$$

$$\text{where} \quad \alpha = V/U \qquad (11)$$

The source of the difference is the u|u| term in (1). The relation between C_M and b_1 is the same as before, and the relation between C_D and a_1 becomes

$$C_D = a_1/2\alpha \qquad (12)$$

When V<U, so that the flow does reverse in each cycle, the relationship between C_M and b_1 is again (8), but the relation between C_D and a_1 becomes

$$C_D = (3\pi/8\beta)a_1 \qquad (13)$$

$$\text{where} \quad \beta = (3\alpha/2)\arcsin\alpha + \tfrac{1}{2}(1-\alpha^2)^{\frac{1}{2}}(2+\alpha^2) \qquad (14)$$

The lift coefficients were evaluated from the extreme values of the lift data. In each measurement run, the maximum lift forces for each flow direction were averaged, and divided by the corresponding averaged maximum value of $\tfrac{1}{2}\rho Du^2$.

The calculated values of C_M, C_D and C_L are plotted as functions of the semi-orbital movement of the water, denoted a, divided by the diameter D. For pure oscillatory motion, a/D is $1/2\pi$ times the Keulegan-Carpenter number UT/D, where T is the period $2\pi/\omega$. When a superimposed steady current V was present, the results were plotted against an equivalent semi-orbital movement a' defined by

$$a' = a(1 + U/a\omega)^2 \qquad (15)$$

Results

Ten different cases were analysed. They are summarised in Figure 1.

The first three cases are a pipe on the bottom, partly buried to 1/4 diameter, and partly buried to 1/2 diameter: to simplify cross-reference these cases are numbered 2 through 4, so that the Figure number for the results is the same as the case number.

Case 5 is a pipe of diameter D in a trench of depth ½D. The trench is V-shaped, with sides at 30° to the horizontal, and is representative of a ploughed trench in dense sand or in a cohesive material such as clay. When the seabed is uneven, the profile of the bottom of the trench is a somewhat smoothed form of the seabed profile (because of the kinematics of a long-beamed plough[4]), but it is still possible for the pipe to span within the trench. It was therefore decided to examine the forces on a pipe spanned above the bottom of the trench: this is done in cases 6 and 7.

Ploughing leaves a spoil mound ("furrow") neatly placed along the sides of the trench. The spoil mound further shelters the pipe, and reduces hydrodynamic forces. This effect is seen in cases 8 9 and 10, for a pipe of diameter D in a trench of depth ½D, on the trench bottom and at heights of 0.2D and ½D above the bottom. The spoil mound cross-section was taken as a sector of a circle, rising to a height of 0.21D above the original seabed: this is a reasonable idealisation of the spoil left by a plough.

Finally, case 11 is a pipe in a trench of depth D.

The results are presented in Figures 2 through 11. Each plots C_D, C_M and C_L against a'/D. The plots distinguish between the tests in which there was no steady current and those in which different levels of steady current were superposed.

It can be seen that there is some scatter in the experimental results. This is invariably found in hydrodynamic experiments in oscillatory flow, and can be attributed to the irregular formation of large vortices in the wake as the water is swept back and forth across the pipe.

Discussion

The results for the pipe on the bottom can be compared with other research. Differences occur because of different experimental techniques, because of different levels of surface roughness, and because of different methods of extracting the coefficients from the data.

Figure 12 compares the relation between C_L and Keulegan-Carpenter number for a pipe on bottom from the present work with the results of Bryndum and Jacobsen[5] and with the coefficients given in the 1981 Det norske Veritas rules[6]. There is a broad agreement in the dependence on Keulegan-Carpenter number, but the present work gives slightly lower values. If the comparison had been on the basis of maximum forces, rather than Fourier coefficients, the agreement would have been closer.

As would be expected, the forces on a pipe partially buried in the seabed are smaller than those on an unburied pipe. Figure 13 shows how C_D, C_M and C_L depend on embedment when a'/D is 6. It also includes C_D and C_L determined from earlier work on drag and lift forces on partially-embedded pipes in a steady current[7].

A trench shelters a pipeline and reduces hydrodynamic forces, and the presence of spoil mounds creates a small further reduction. Figure 14 shows how C_D, C_M and C_L depend on trench depth when a'/D is 6.

If there is a gap under a pipe in a trench (cases 6 7 9 and 10), the top of the pipe extends further above the bottom, which tends to increase the drag, but water can pass under the pipe, which tends to reduce the drag. The net effect on C_D and C_L is relatively small, but C_M falls towards its free-stream potential theory value of 2 as the effect of the boundary is reduced. Even at a gap of ½D, however, the flow around the pipe is still influenced by the presence of the trench, and the lift forces are higher than they are for a pipe spanned at a height of ½D above an undisturbed seabed.

Stability in a trench

The stability of a marine pipeline depends both on the hydrodynamic forces and on the lateral resistance mobilised by the seabed. Remarkably, far more attention has been given to the hydrodynamic problem than to the equally important geotechnical one, though this discrepancy is at long last being corrected by new research in Norway[8,9] and Denmark.

It is traditional to adopt an extremely simple idealisation of the geotechnical interaction between a pipeline and the seabed, and to treat it as a contact governed by Coulomb friction. The limiting value of the tangential reaction S between the pipe and the bottom is taken as the current value of the normal reaction R multiplied by a "friction coefficient" f. This idealisation can be criticised from the viewpoint of geotechnics, but recent research shows it to be a reasonable representation of the results of tests on pipes resting on sand without any significant embedment. If the pipe is embedded in the bottom, even to a small extent, the frictional model is inadequate, particularly if the loading is cyclic.

Even applying the simple Coulomb idealisation, a trench markedly increases lateral stability, by a second effect independent of hydrodynamic sheltering. This can be seen in Figure 15, which compares a pipe on a level bottom with a pipe in a trench with side slope θ. The angle of friction is ϕ, so that

$$\phi = \arctan f \tag{16}$$

For the pipe on a level bottom

$$S = F_x \tag{17}$$

$$R = w - F_y \tag{18}$$

and the pipe begins to slide when

$$\tan \phi = S/R = F_x/(F_y - w) \tag{19}$$

For the pipe in a trench

$$S = F_x \cos\theta - (w - F_y)\sin\theta \tag{20}$$

$$R = F_x \sin\theta + (w - F_y)\cos\theta \tag{21}$$

and the pipe begins to slide when

$$\tan\phi = S/R \tag{22}$$

which rearranges into

$$\tan(\phi+\theta) = F_x/(w-F_y) \tag{23}$$

Comparison shows that the effect of the trench is to replace the friction coefficient f by $\tan(\phi+\theta)$, which is usually much larger than f. If, for instance, f is taken as 0.70, so that ϕ is arctan(0.7) which is 35°, and the trench side slope θ is 30°, the effective friction coefficient is tan(65°) which is 2.1.

The above model assumes that the pipe becomes unstable by sliding up the side of the trench. In principle, it could move sideways by deforming the trench sides. In practice, even a very small shear strength in the bottom soil is enough to prevent this. If the trench sides are composed of a soil which can be treated as a ideal plastic material, the force F_R per unit length required to deform the trench sides is approximately

$$F_R = cH[8/\sqrt{3} + (\gamma H/c)/2\sqrt{3}] \tag{24}$$

where
- c is the undrained shear strength of the soil
- H is the trench depth
- γ is the submerged unit weight of the soil

The ratio between the drag component of the horizontal force and the horizontal resistance to trench side deformation is therefore

$$F_x'/F_R = \tfrac{1}{2}C_D\rho DU^2/cH[8/\sqrt{3} + (\gamma H/c)/2\sqrt{3}] \qquad (25)$$

If, for instance, ~~k~~ c (surely) is 3 kPa and γ is 8 kN/m³ (typical values for a very soft marine clay), U is 1 m/s, ρ is 1025 kg/m³, D is 1 m, H is 0.5 m and C_D is 0.6, this ratio is only 0.04 and there is a large margin of safety against deforming the trench.

Conclusion

The test results reported in this paper provide a basis for the stability design of pipelines in trenches.

Acknowledgements

The authors thank British Petroleum and Woodside Petroleum for permission to publish this paper.

References

1 Wave and current forces on pipelines in trenches and part buried. Hydraulics Research Station, report EX1012 (1981).

2 Grace, R.A., Andres, J.M. and Lee, E.K.S. Forces exerted by shallow ocean waves on a rigid pipe set at an angle to the flow. Proceedings, Institution of Civil Engineers, 83, 43-59 (1987).

3 Sarpkaya, T. and Isaacson, M. Mechanics of Wave forces on Offshore Structures. Van Nostrand Reinhold, New York (1981).

4 Brown, R.J. and Palmer, A.C. Submarine pipeline by multi-pass ploughs. Proceedings, Seventeenth Annual Offshore Technology Conference (Houston), 2, 283-291 (1985).

5 Bryndum, M. B. and Jacobsen, V. Hydrodynamic forces from wave and current loads on submarine pipelines, Proceedings, Fifteenth Annual Offshore Technology Conference (Houston), 1, 95-102 (1983).

6 Rules for submarine pipeline systems, Det norske Veritas, Hovik, Norway (1981).

7 Littlejohns, P.S.G. Current-induced forces on submarine pipelines, Hydraulics Research Station, Wallingford, England, report INT 138 (1974).

8 Brennoden, H., Sveggen, O., Wagner, D.A. and Murff, J.D. Full-scale pipe-soil interaction tests, Proceedings, Eighteenth Annual Offshore Technology Conference, OTC 5338, 4, 433-440 (1986).

9 Wagner, D.A., Murff, J.D., Brennoden, H. and Sveggen, O. Pipe-soil interaction model. Proceedings, Nineteenth Annual Offshore Technology Conference, OTC 5504, 3, 181-190 (1987).

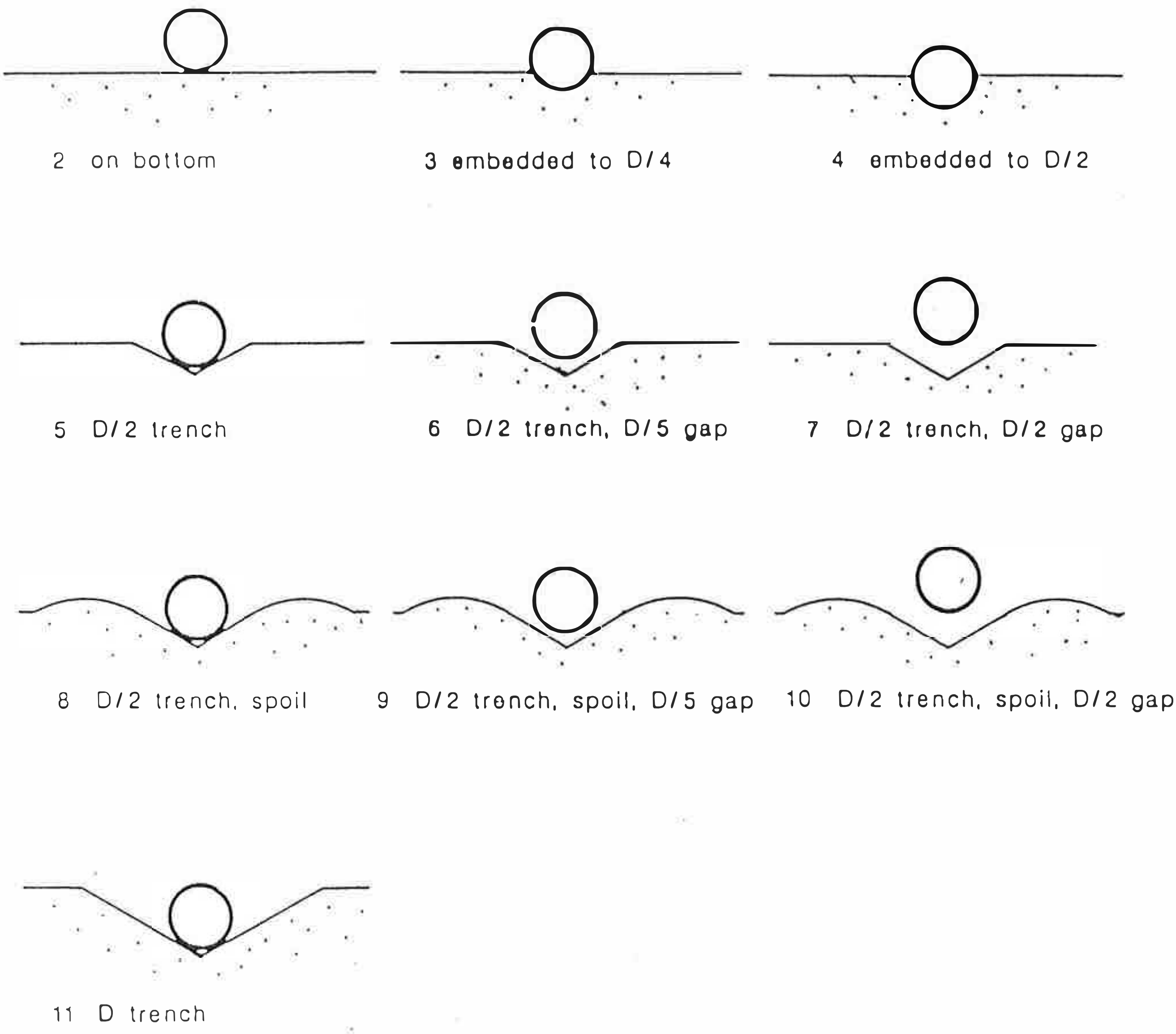

D is pipe outside diameter

numbers refer to Figures where C_D C_M and C_L are given

CASES TESTED

FIGURE 1

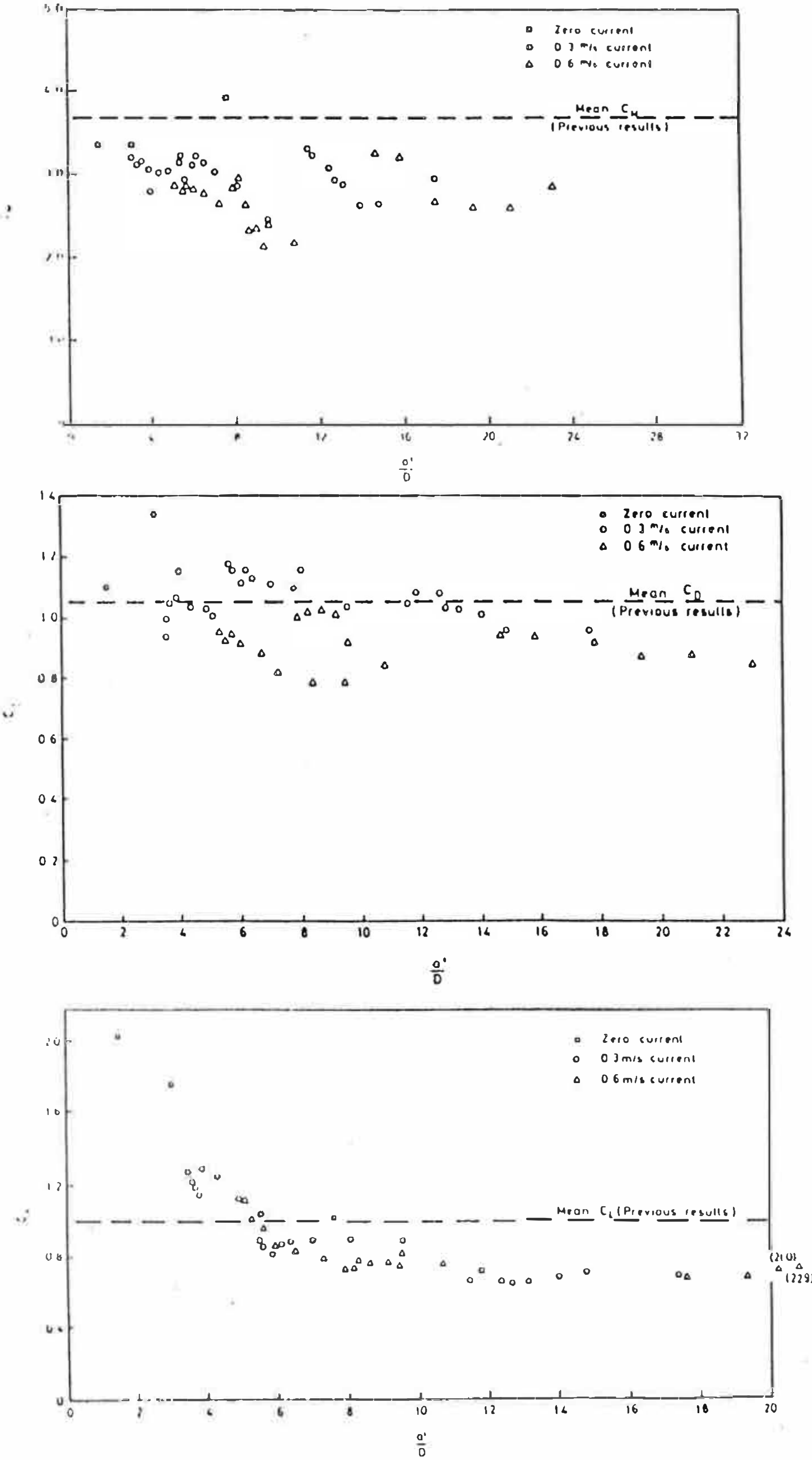

note: scales on a'/D axes differ

case 2: on bottom

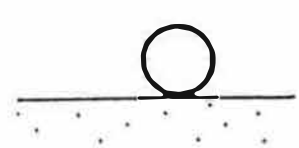

HYDRODYNAMIC COEFFICIENTS

FIGURE 2

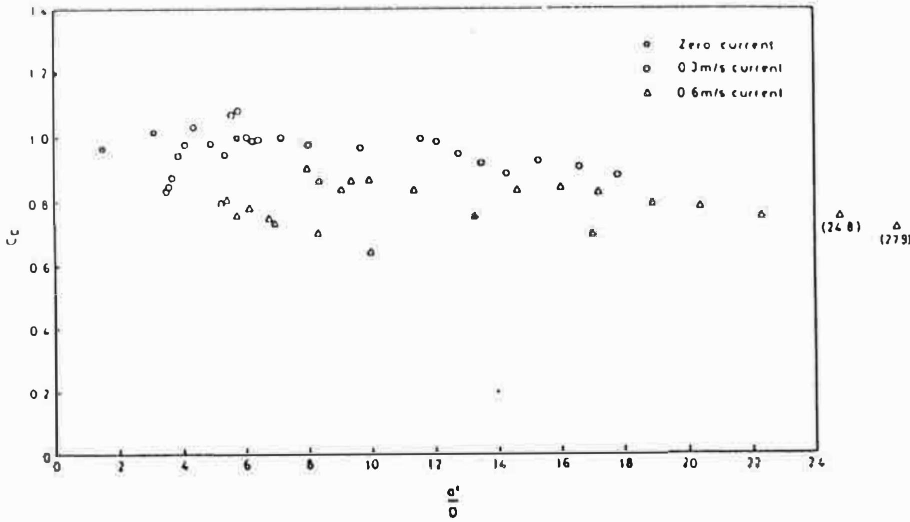

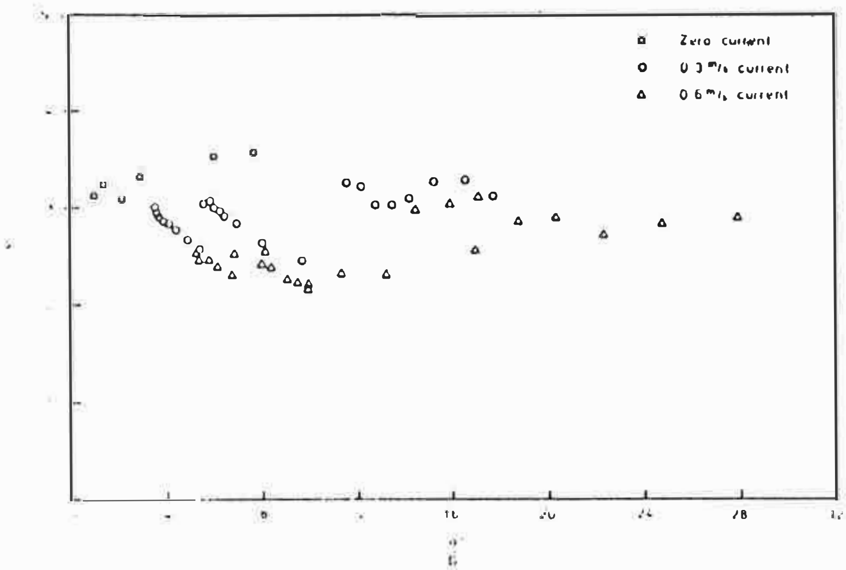

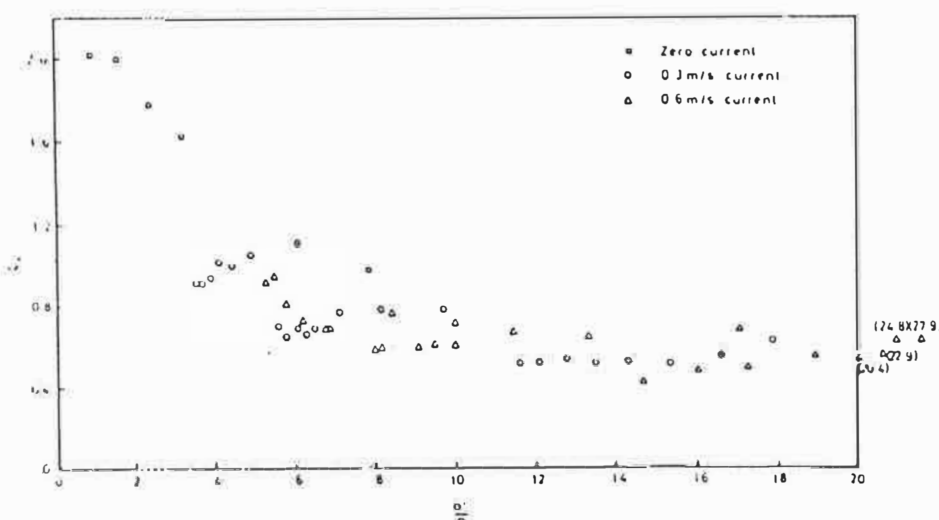

note: scales on a'/D axes differ

case 3: embedded to D/4

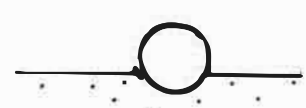

HYDRODYNAMIC COEFFICIENTS

FIGURE 3

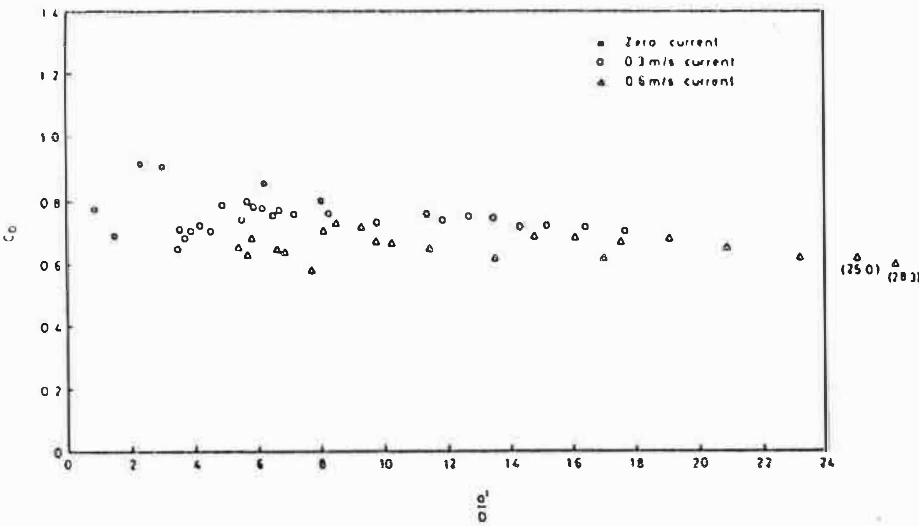

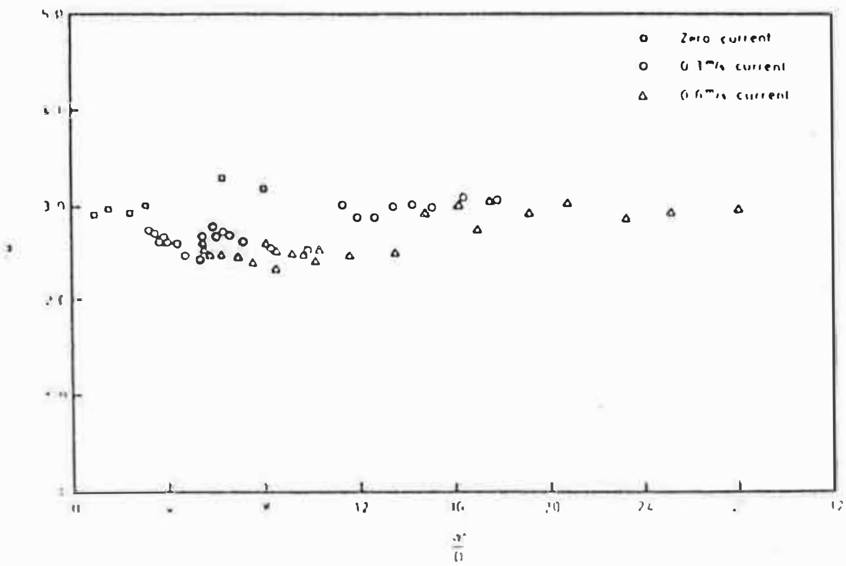

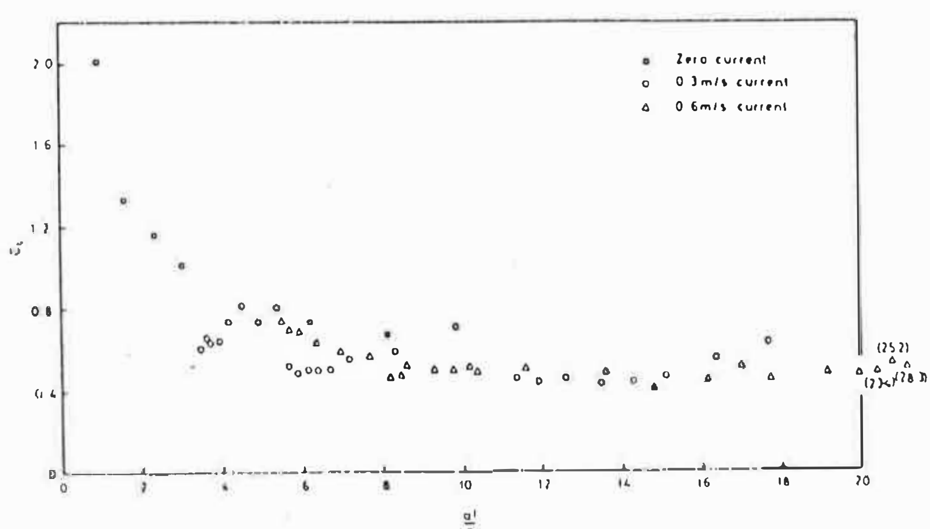

note: scales on a'/D axes differ

case 4: embedded to D/2

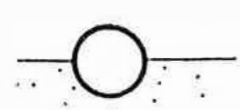

HYDRODYNAMIC COEFFICIENTS

FIGURE 4

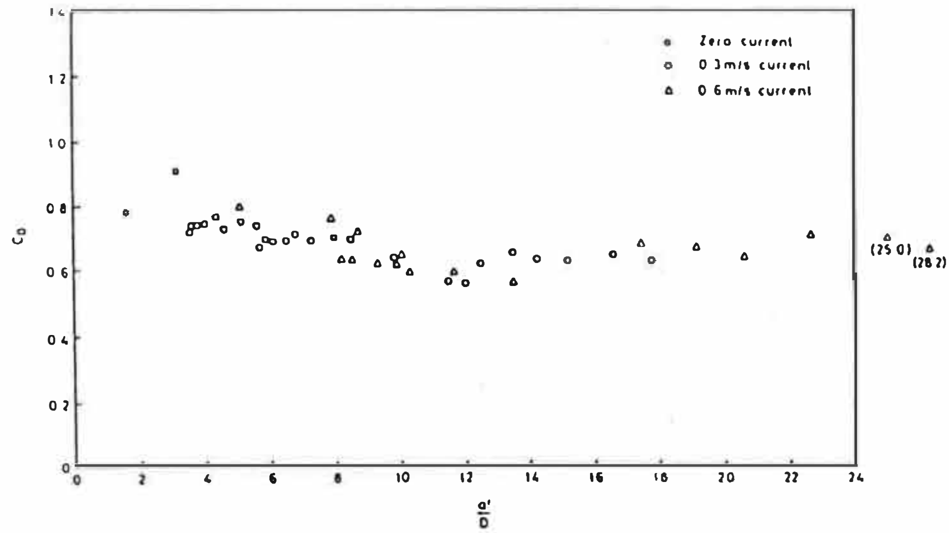

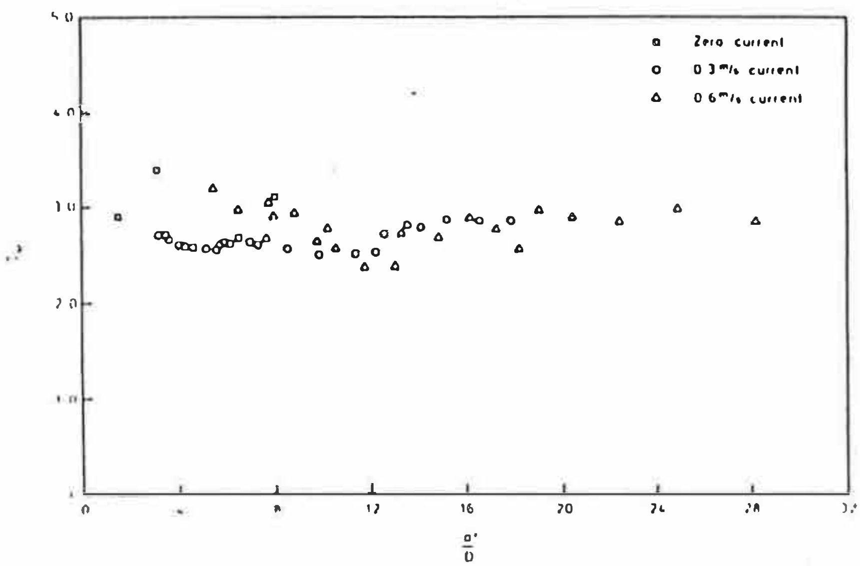

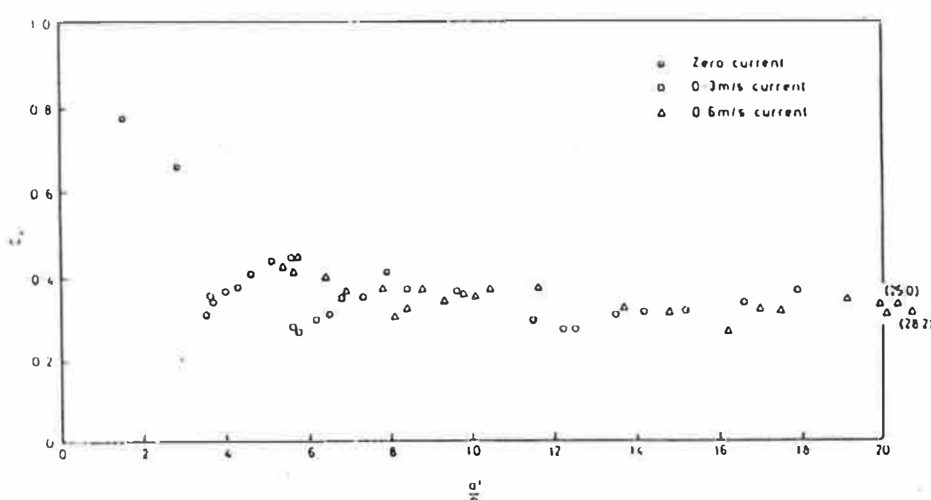

note: scales on a'/D axes differ

case 5: trench D/2

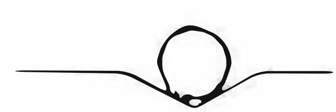

HYDRODYNAMIC COEFFICIENTS

FIGURE 5

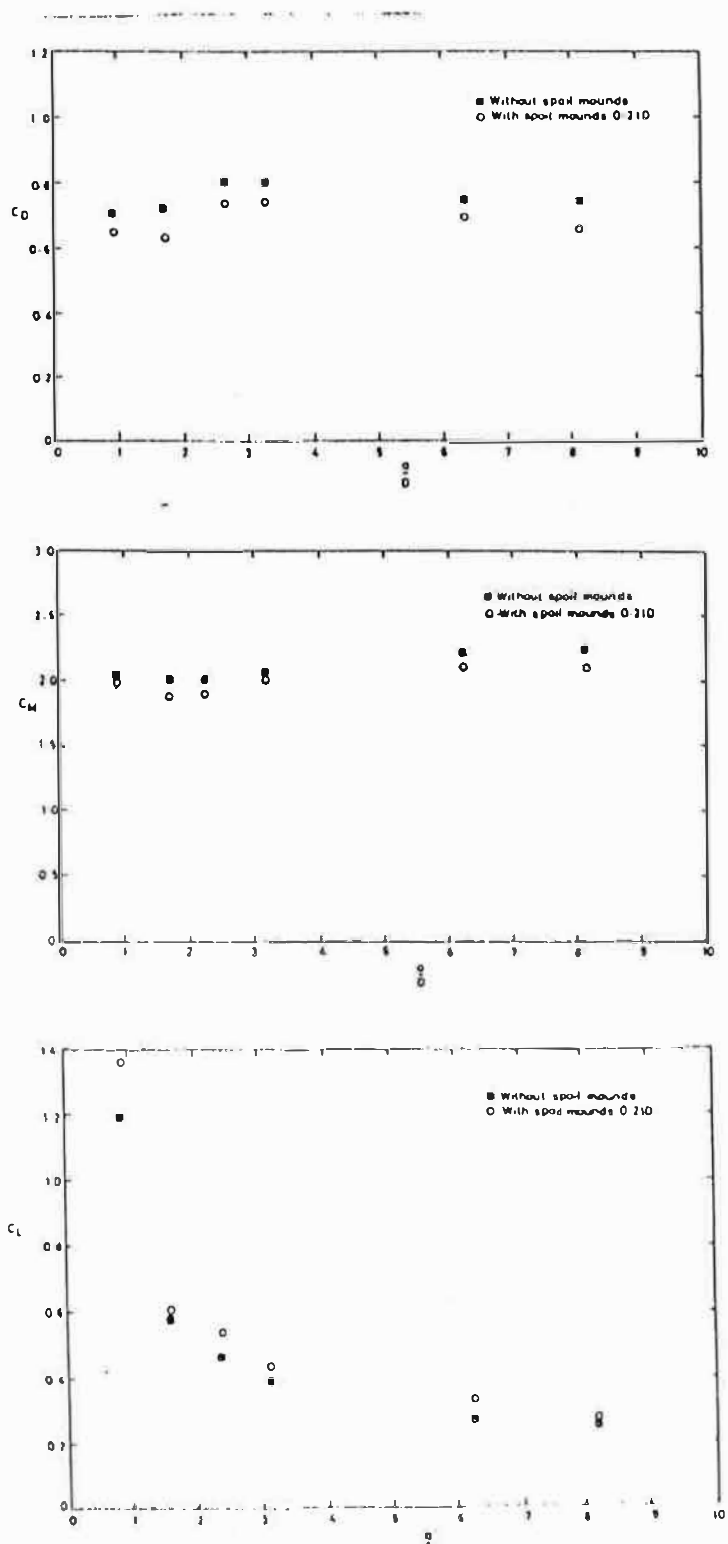

case 6: trench D/2, gap D/5

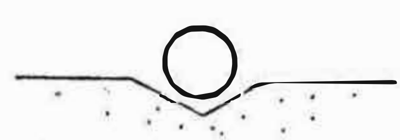

HYDRODYNAMIC COEFFICIENTS

FIGURE 6

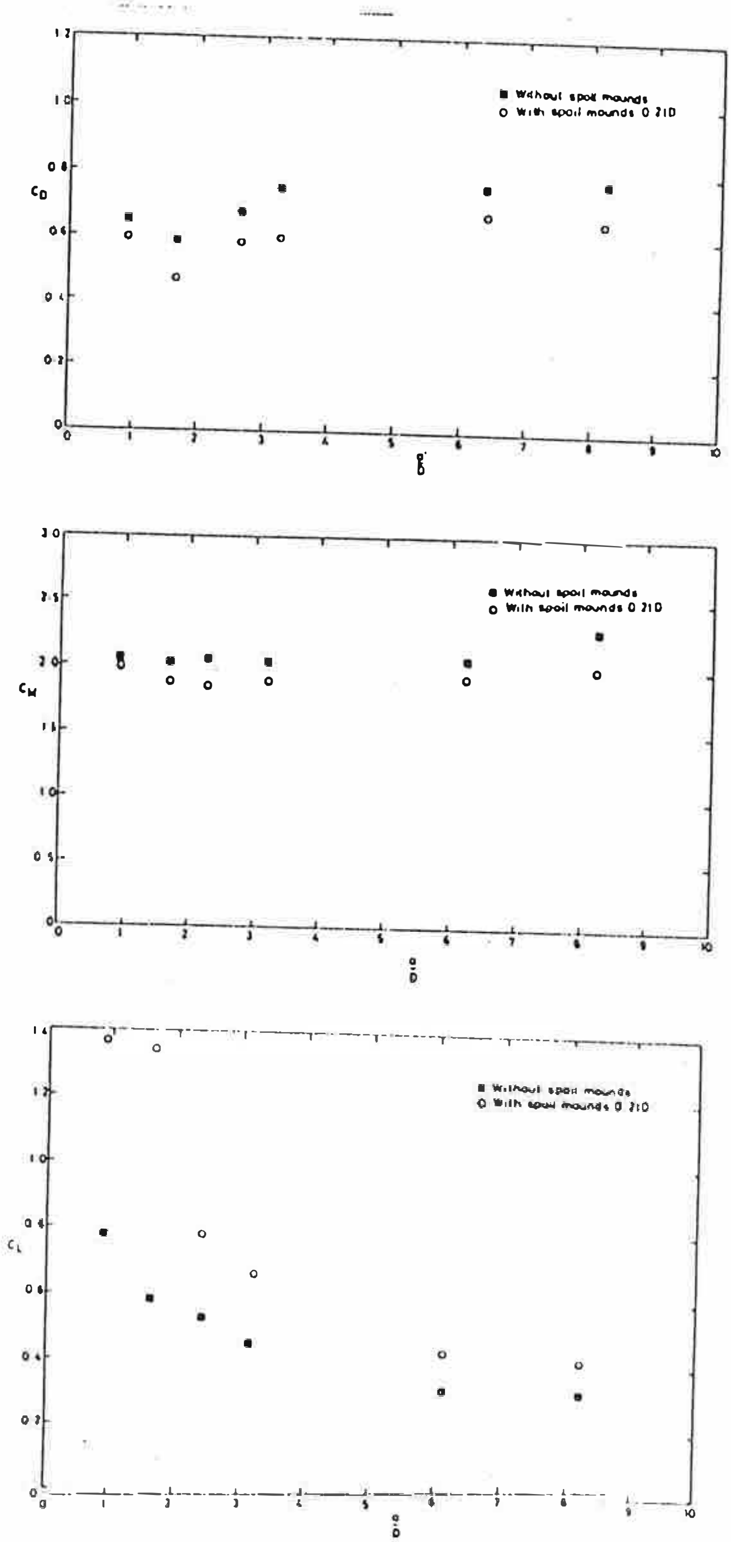

case 7: trench D/2, gap D/2

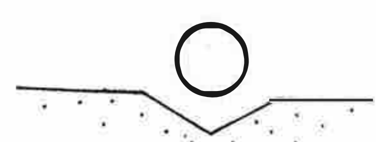

HYDRODYNAMIC COEFFICIENTS

FIGURE 7

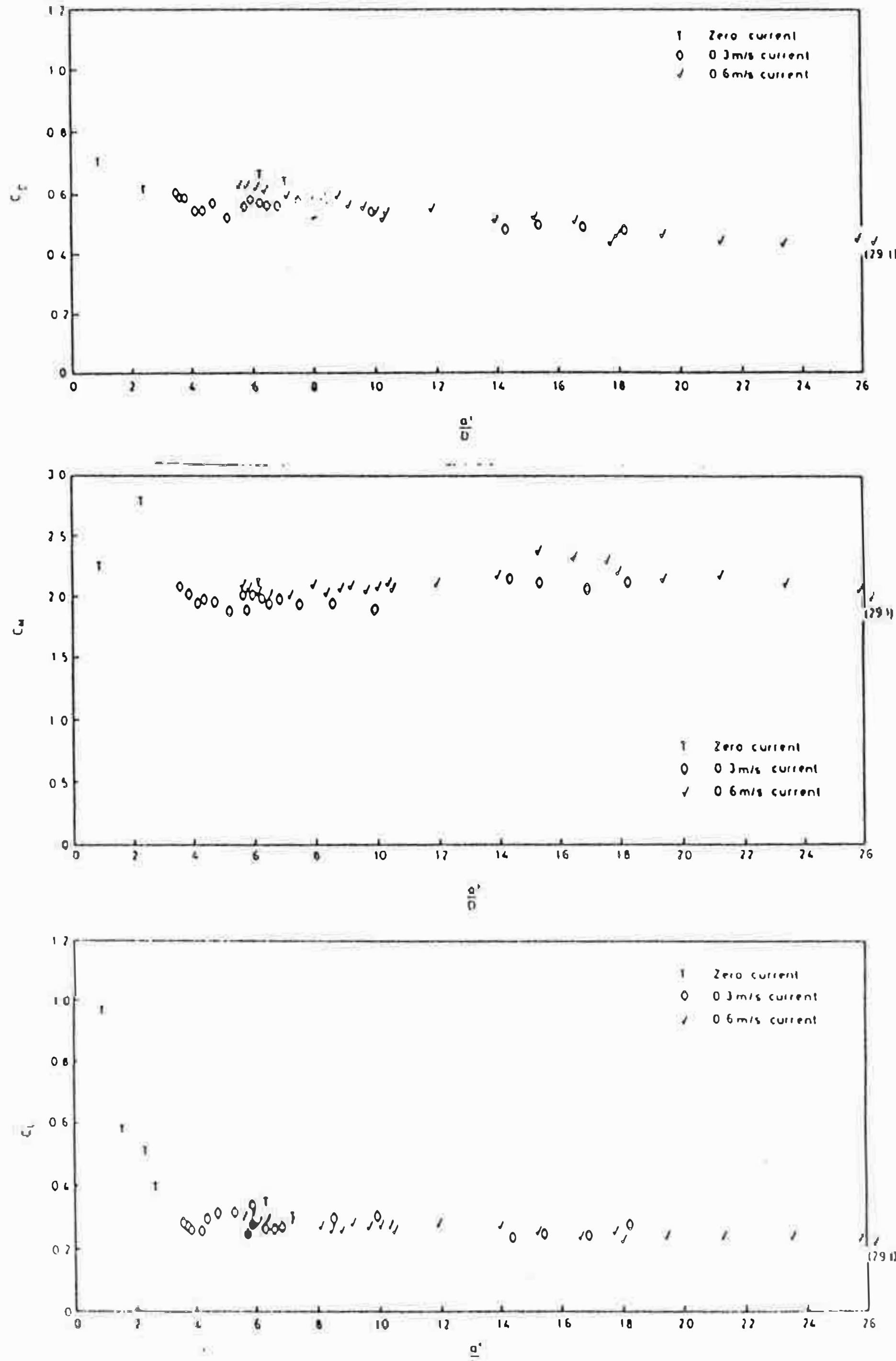

case 8: trench D/2, spoil

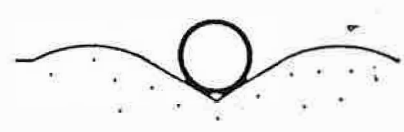

HYDRODYNAMIC COEFFICIENTS

FIGURE 8

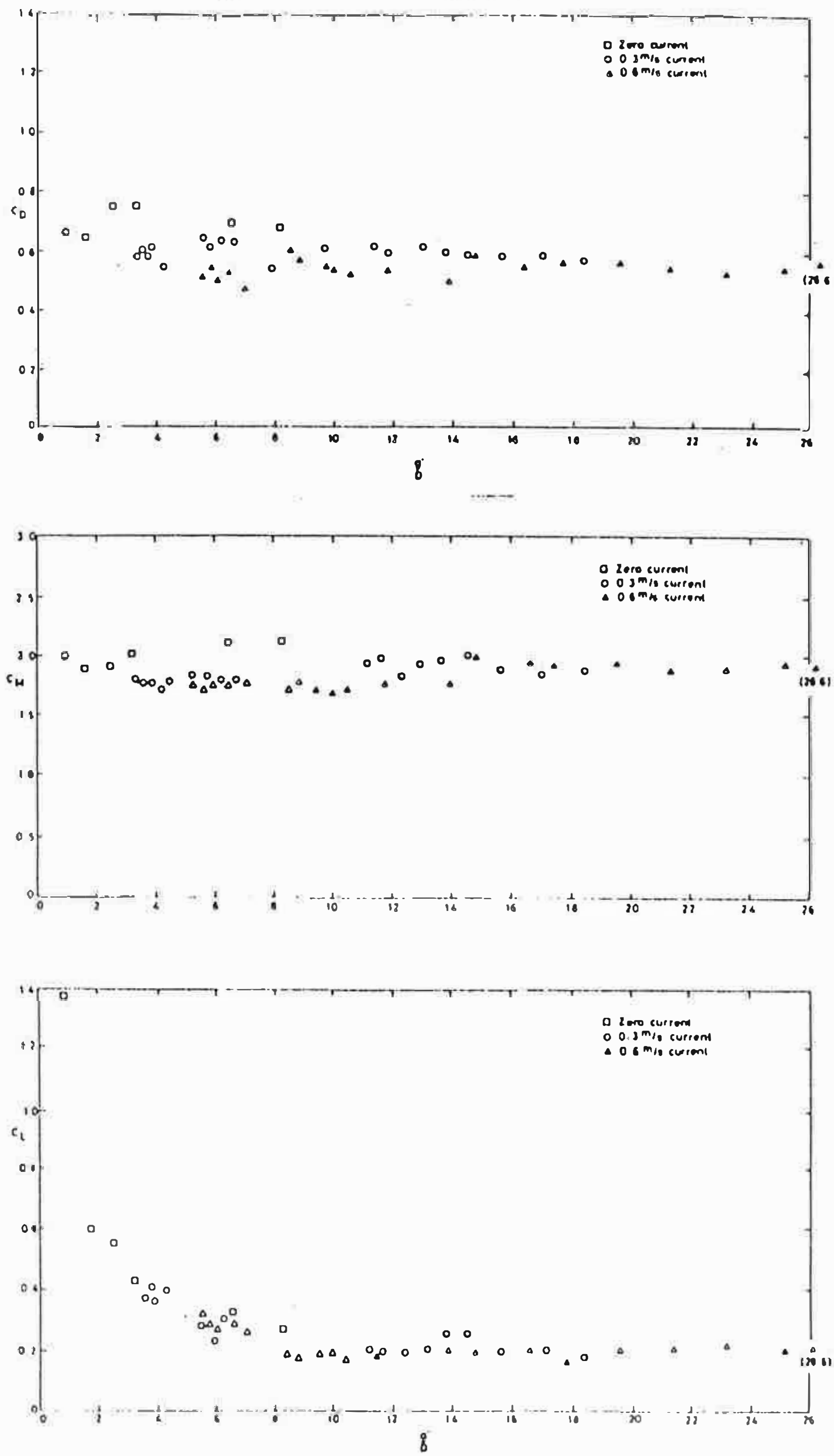

case 9: trench D/2, spoil, gap D/5

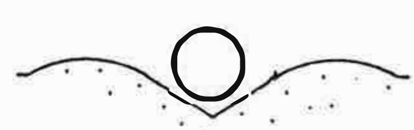

HYDRODYNAMIC COEFFICIENTS

FIGURE 9

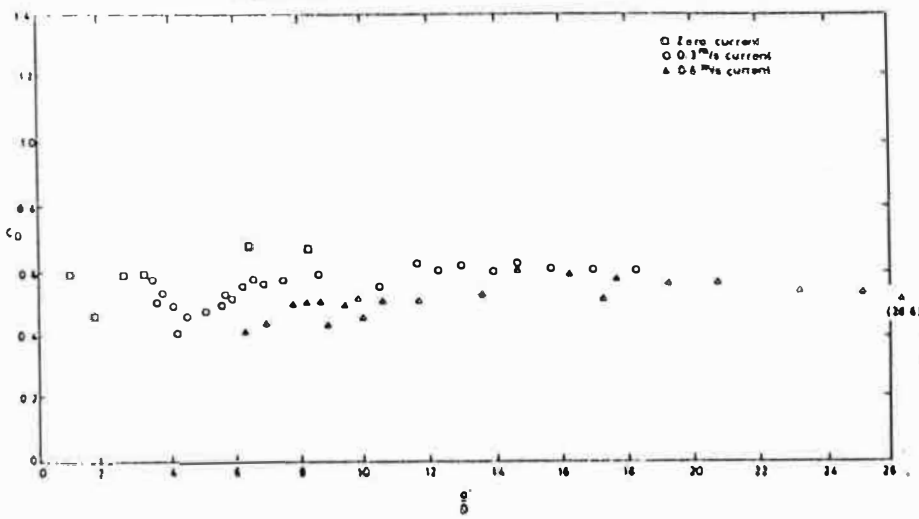

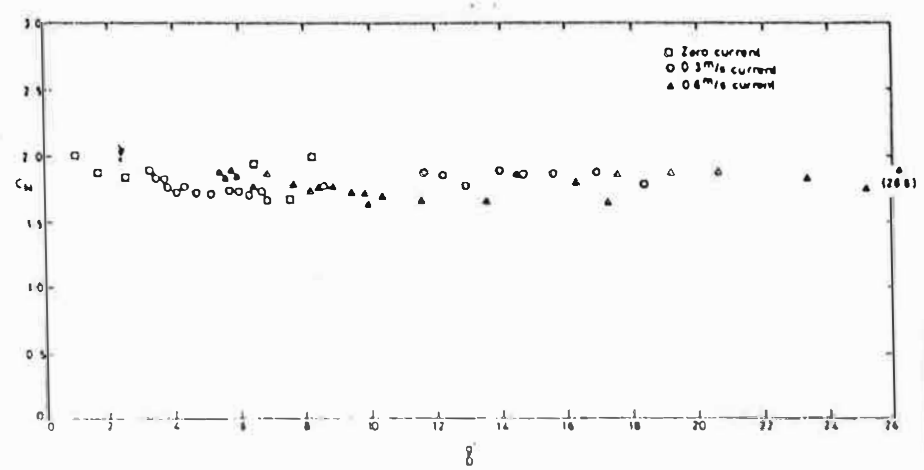

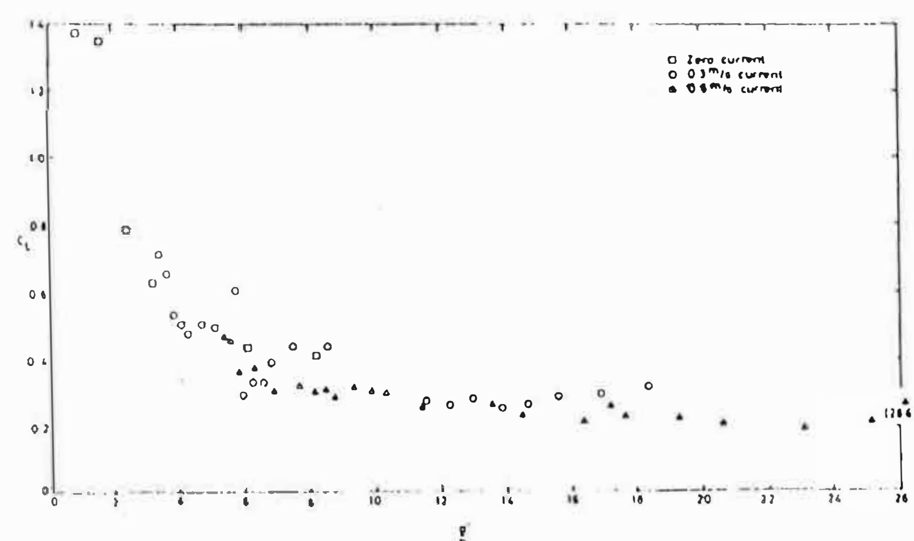

case 10: trench D/2, spoil, gap D/2

HYDRODYNAMIC COEFFICIENTS

FIGURE 10

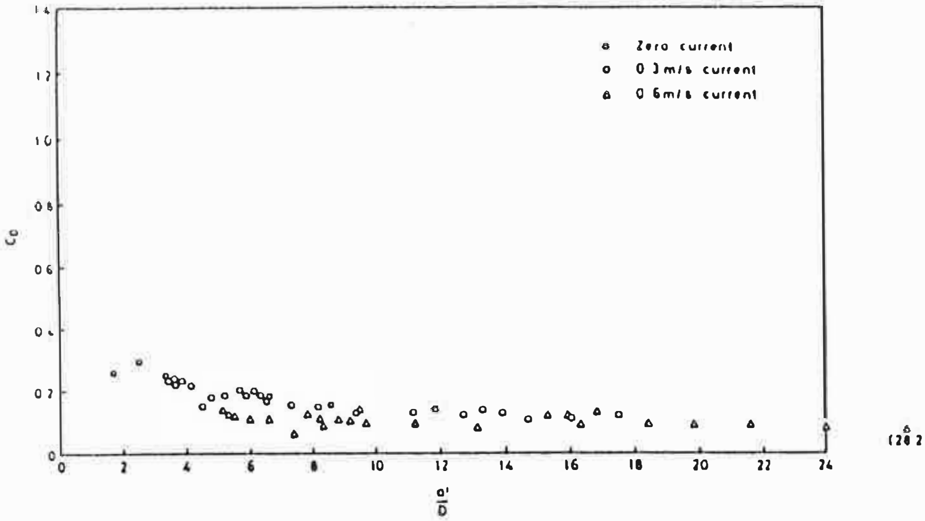

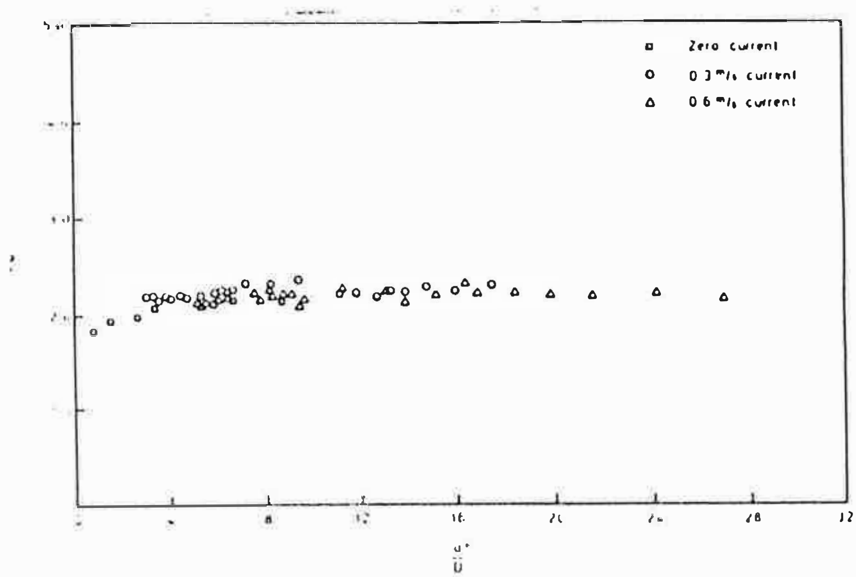

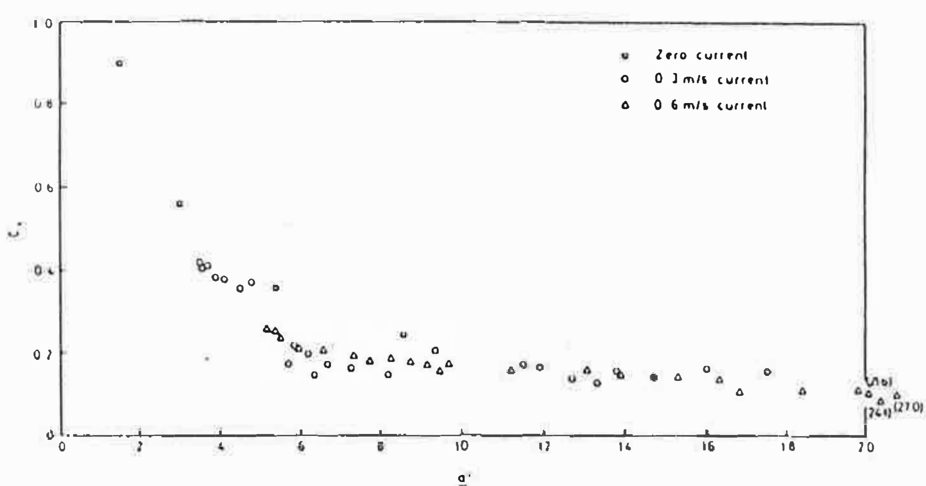

note: scales on a'/D axes differ

case 11: trench D

HYDRODYNAMIC COEFFICIENTS

FIGURE 11

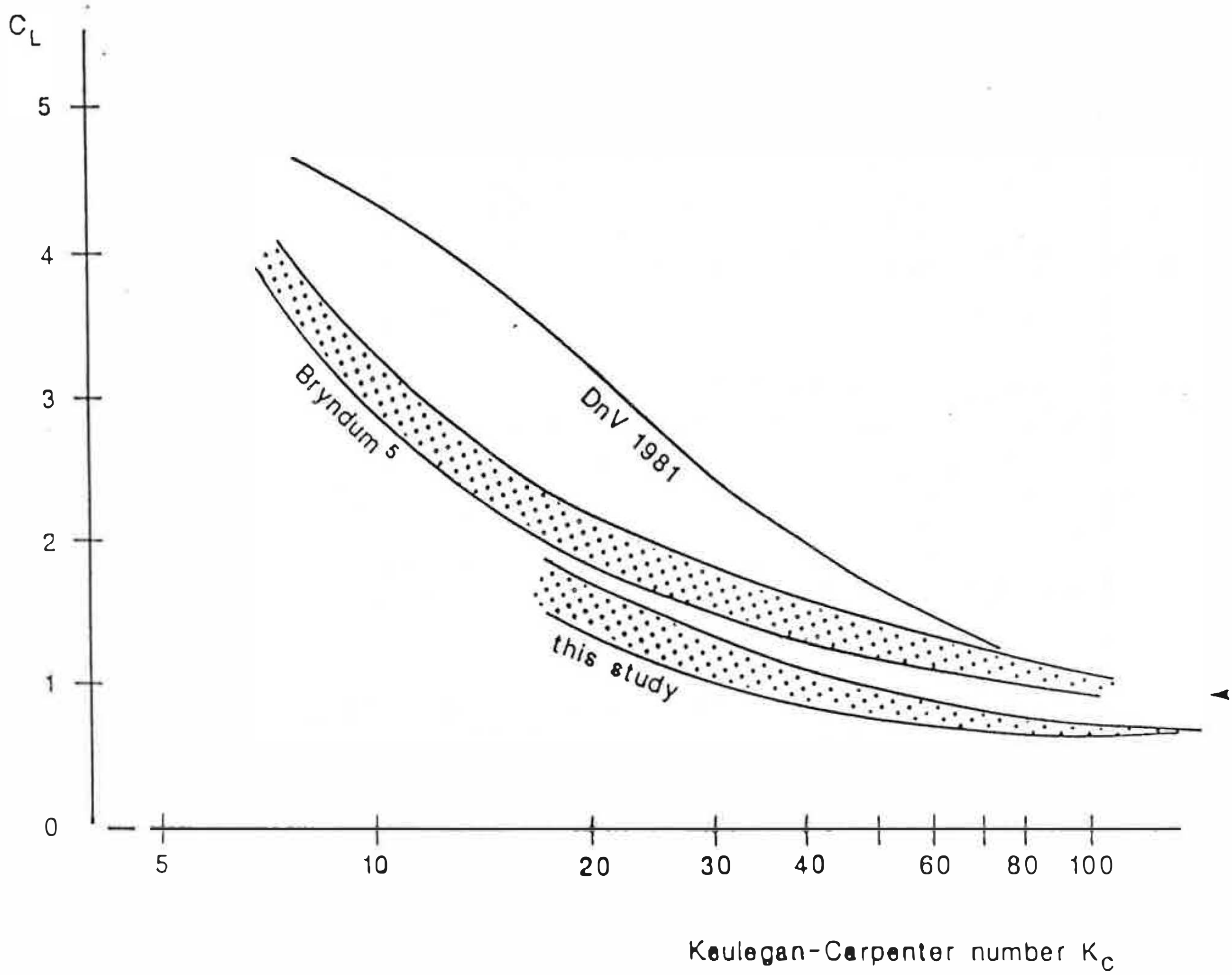

◄ smooth pipe in steady current at high Reynolds number[7]

COMPARISON OF LIFT COEFFICIENTS

FIGURE 12

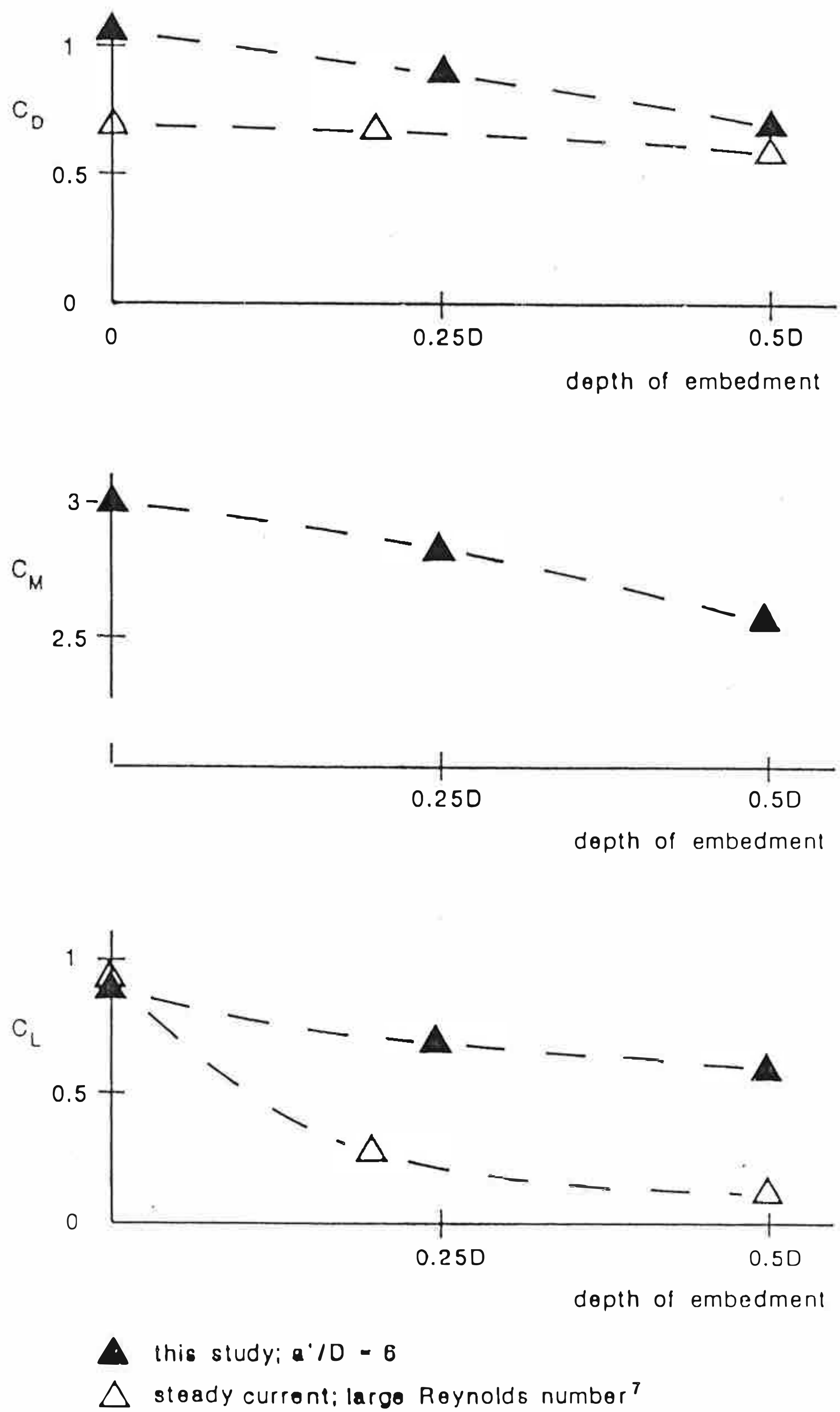

EFFECT OF EMBEDMENT

FIGURE 13

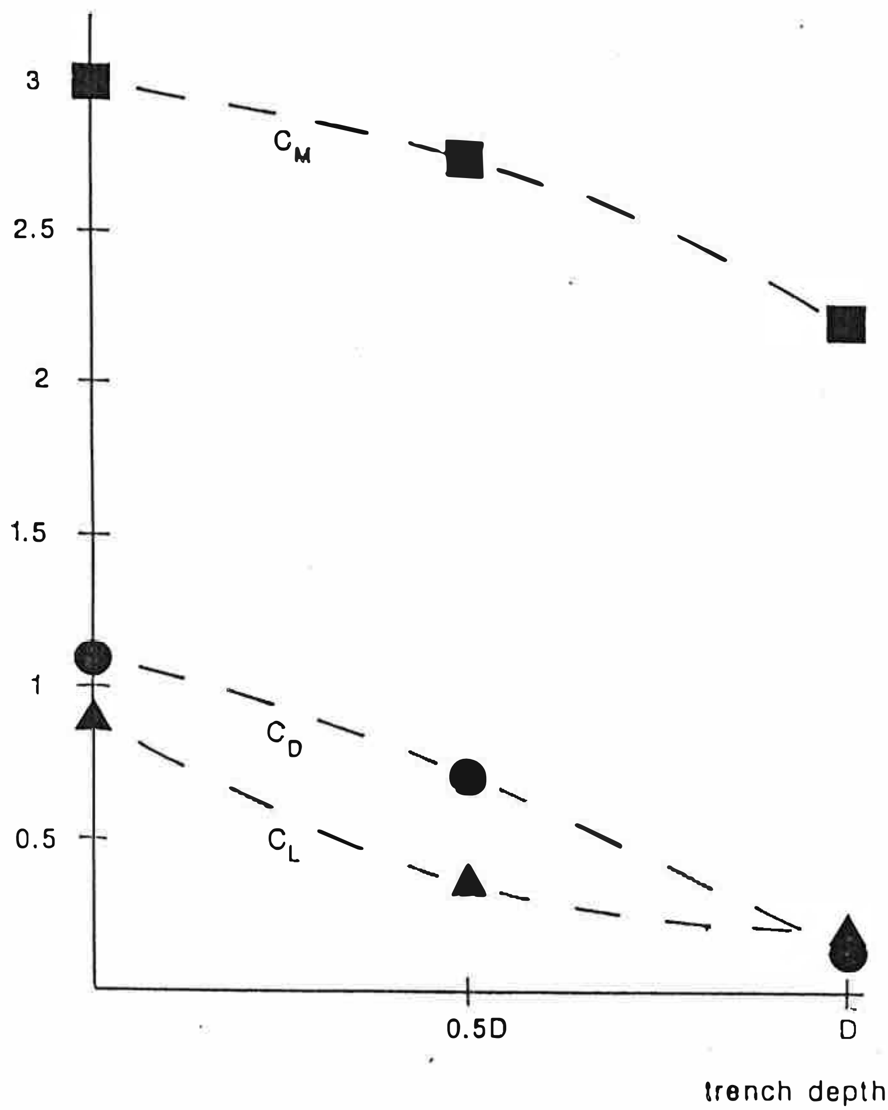

.EFFECT OF TRENCH DEPTH

FIGURE 14

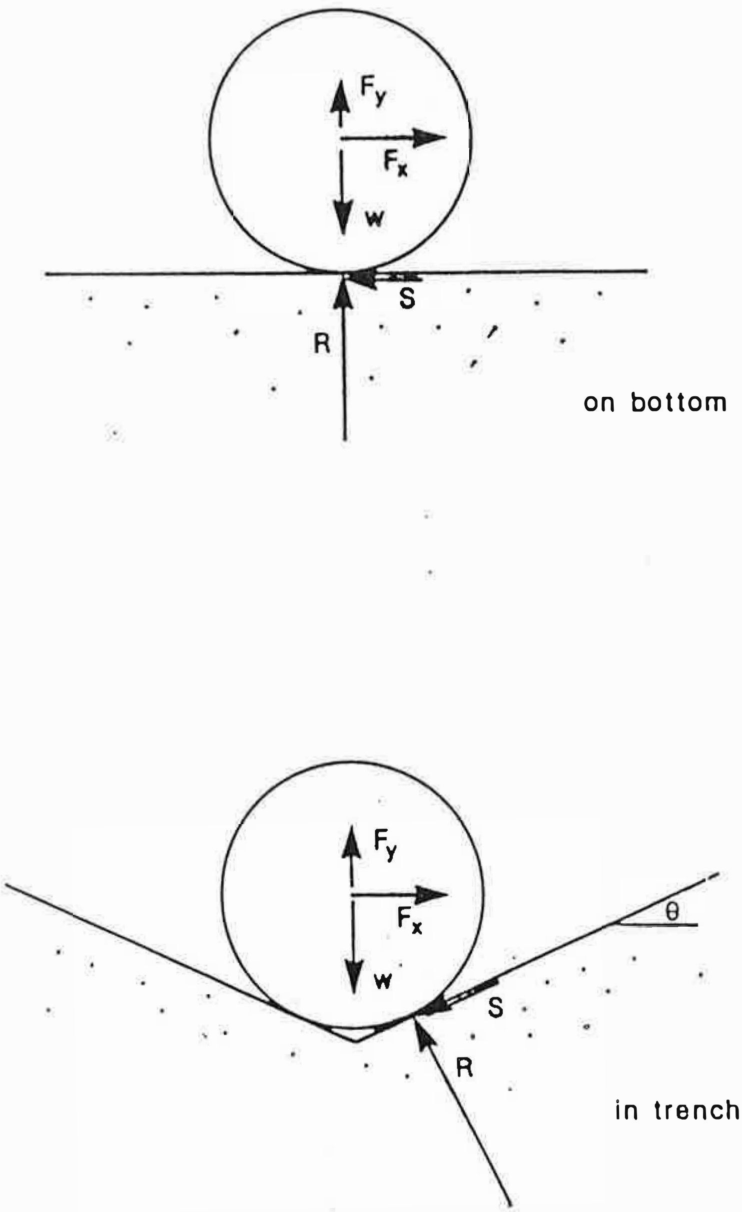

LATERAL RESISTANCE IN A TRENCH : COULOMB MODEL

FIGURE 15